

Parity Alternation of Ground-State P_n^- and P_n^+ ($n = 3–15$) Phosphorus Clusters

M. D. Chen,* Q. B. Chen, J. Liu, L. S. Zheng, and Q. E. Zhang

State Key Laboratory for Physical Chemistry of Solid Surfaces, Department of Chemistry, Center for Theoretical Chemistry, College of Chemistry and Chemical Engineering, Xiamen University, Xiamen 361005, People's Republic of China

C. T. Au

Department of Chemistry, Hong Kong Baptist University, Kowloon Tong, Hong Kong, People's Republic of China

Received: October 23, 2006; In Final Form: November 13, 2006

The ground-state structures of neutral, cationic, and anionic phosphorus clusters P_n , P_n^+ , and P_n^- ($n = 3–15$) have been calculated using the B3LYP/6-311+G* density functional method. The P_n^+ and P_n^- ($n = 3–15$) clusters with odd n were found to be more stable than those with even n , and we provide a satisfactory explanation for such trends based on concepts of energy difference, ionization potential, electron affinity, and incremental binding energy. The result of odd/even alternations is in good accord with the relative intensities of cationic and anionic phosphorus clusters observed in mass spectrometric studies.

1. Introduction

During the past decade, much research has been directed toward understanding the structures and properties of small carbon clusters.¹ Recently, there has been renewed interest in the study of phosphorus clusters. The fact that elemental phosphorus has a large variety of structures has been known for many years.² In the form of clusters, phosphorus displays endless varieties as well as structures. It has been reported that laser ablation of elemental phosphorus in connection with time-of-flight (TOF) mass spectrometry leads to the formation of singly charged P_n^+ and P_n^- clusters.^{3–9}

Because of their potential applications, phosphorus clusters have been investigated theoretically for a long time. Lin et al. proposed structures of P_n^+ clusters based on data collected by ab initio calculations.⁴ Ahlrichs et al. carried out a theoretical study on the stability of molecular P_2 , P_4 , and P_8 using ab initio calculations.¹⁰ Jones and co-workers investigated structures of neutral, cationic, and anionic phosphorus clusters using the simulated annealing method.^{11–14} Häser et al. performed ab initio SCF and MP2 calculations to study a variety of neutral phosphorus clusters up to P_{28} .^{15–17} Warren and Gimarc investigated P_8 clusters by the SCF molecular orbital approach.^{18–19} Feng and co-workers analyzed P_{2n+1}^+ ($n = 4–6$) and neutral P_n ($n = 6, 10, 12, 14, 32$) clusters at the HF/6-31G* level.^{20–25} Guo et al. conducted B3LYP/6-311G(d) density functional calculations on the geometric and electronic properties of neutral, cationic, and anionic P_n ($n = 3–15$) clusters.²⁶ Han et al. carried out DFT and HF investigations on fullerene-like phosphorus clusters.²⁷ Wang et al. carried out a comparative study on the structures and electron affinities of P_n and P_n^- ($n = 1–6$) species by means of seven DFT methods.²⁸ We performed theoretical calculations on the structures of P_n^+ and P_n^- ($n = 5, 7, 9, 11$), and P_n ($n = 5–13$).^{29–35} To interpret the mass spectrum of P_n^+ , we constructed structures of large P_n^+

clusters (from P_{25}^+ to P_{89}^+) based on the assumption that the large clusters could be built from P_8 units.³⁶

Figures 1 and 2 show the TOF mass spectra of cationic and anionic clusters, respectively.⁵ In these figures, the cationic and anionic phosphorus clusters show a distinct even/odd pattern of intensity variation: The signals of odd- n clusters are more intense than those of even- n clusters. Such a pattern of odd/even variation implies that the clusters with odd numbers of atoms are higher in abundance. To explore this issue further, we recalculated the ground-state structures of P_n , P_n^+ , and P_n^- ($n = 3–15$) phosphorus clusters by means of the B3LYP density functional method. The geometric structures, energy differences, ionization potentials, electron affinities, and incremental binding energies of the phosphorus clusters were examined. In accordance with the results, we provide an explanation for the greater stability of P_n^+ and P_n^- ($n = 3–15$) structures with odd n compared to those with even n . These results are guiding factors for future theoretical studies on large phosphorus clusters. The knowledge acquired in this respect can provide helpful information for the synthesis of a variety of novel cluster-assembled materials and can extend our understanding of the nature of novel cluster materials.

2. Computational Method

In the investigation of ground-state clusters, we performed molecular graphics, molecular mechanics, and quantum chemistry calculations. First, a three-dimensional model of a cluster was designed using HyperChem for Windows³⁷ and Desktop Molecular Modeller for Windows³⁸ on a PC/Pentium IV computer. Then, the model was optimized by MM+ molecular mechanics and semiempirical PM3 quantum chemistry. At the final stage, geometry optimization and calculations of vibration frequencies were conducted using the B3LYP density functional method of the Gaussian 98 package³⁹ with 6-311G* basis sets, i.e., Becke's three-parameter nonlocal exchange functional with the correlation functional of Lee–Yang–Parr.^{40,41} Single-point energy calculations following the optimizations were performed

* To whom correspondence should be addressed. E-mail: mdchen@xmu.edu.cn.

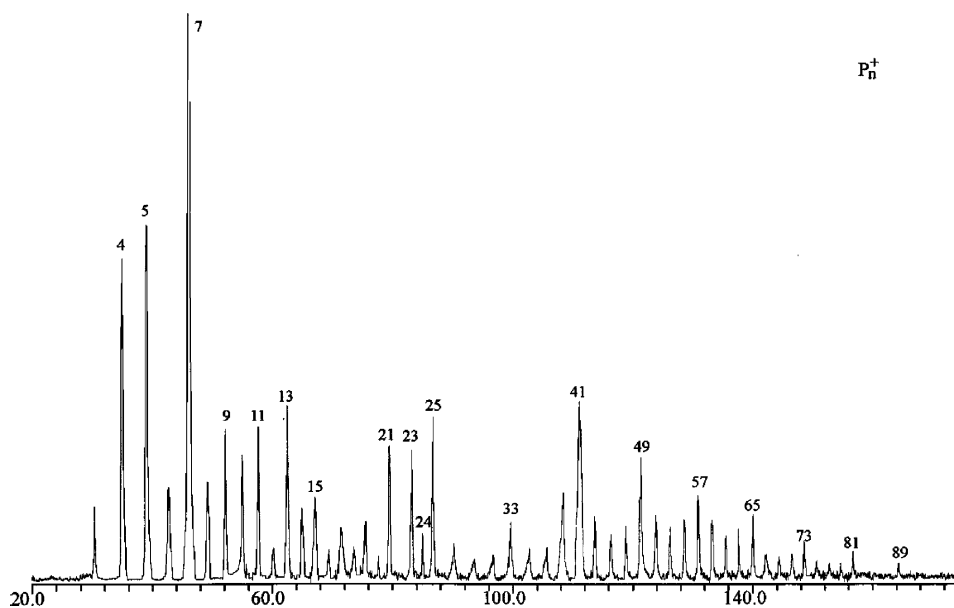


Figure 1. Time-of-flight mass spectrum ($t/\mu\text{s}$) of cationic phosphorus clusters. (The marked values represent the numbers of phosphorus atoms.)

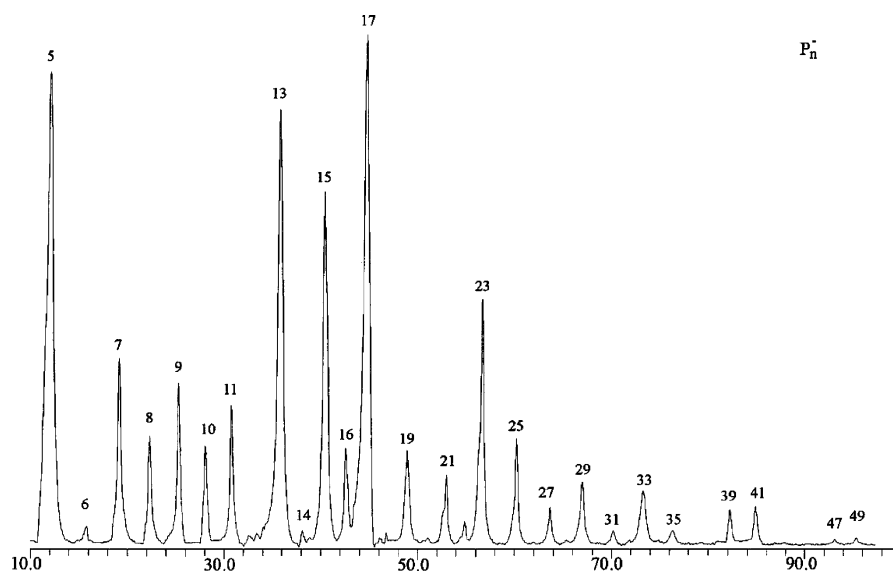


Figure 2. Time-of-flight mass spectrum ($t/\mu\text{s}$) of anionic phosphorus clusters. (The marked values represent the numbers of phosphorus atoms.)

using the larger 6-311+G* basis set, including diffuse functions. The ground-state phosphorus clusters published were scrutinized at the B3LYP/6-311+G**/B3LYP/6-311G* level. Because the change in zero-point energy (ZPE) was only slightly affected by the quality of the employed method, all energies were calculated with the ZPE correction at the B3LYP/6-311G* level.⁴² Calculations with the higher spin multiplicities (triplet or quadruplet) were carried out to guarantee that the lowest-energy configurations were obtained. After the total energies of the clusters had been compared, those configurations with high energy were excluded, and ground-state clusters were determined. The final models were again displayed using HyperChem for Windows. All of the calculations were carried out on SGI servers.

3. Results and Discussion

3.1 Geometry and Energy. Because the numbers of isomers of large clusters are high, it is essential to identify the ground-state structures. For a particular family of molecules, the basic structure with the lowest energy affects the “building up” of larger molecules, and this is an important area in biochemical

research. Although the isomers of cationic, anionic, and neutral phosphorus clusters have been studied extensively and reported in the literature, there can be no guarantee that the global minima have been identified correctly. This is because the energy surface of a large molecule can be rather complex and it is difficult to explore all of the stable minima corresponding to the geometries being considered.⁴³

With co-workers, Jones and Häser investigated the structures of neutral, cationic, and anionic phosphorus clusters using MD and ab initio methods.^{11–17} From a suitable original model, the MD calculation can normally direct an investigator toward global minima. However, if the number of models constructed is not sufficiently large, the ground-state isomers could be missed. Guo et al. performed a theoretical study of the geometric and electronic properties of P_n , P_n^+ , and P_n^- ($n = 3–15$) at the B3LYP/6-311G* level and claimed the correct identification of ground-state geometries of the phosphorus clusters.²⁶ However, we found that many of the ground-state structures determined by Guo et al. are wrong in configuration by comparing the total energies at the same calculation level (B3LYP/6-311G*). The ground-state structures of P_3 , P_6 , P_{10} ,

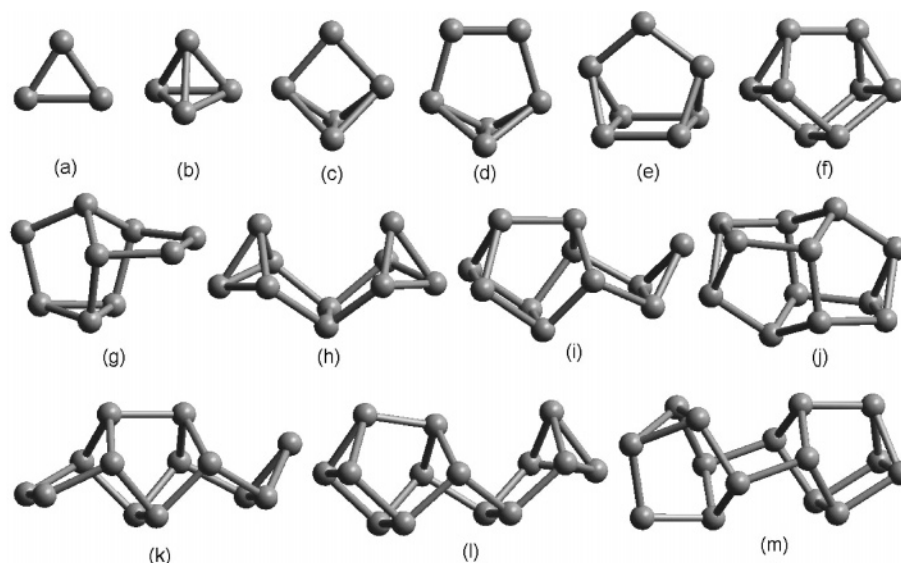


Figure 3. Ground-state geometries of neutral phosphorus clusters P_n ($n = 3-15$).

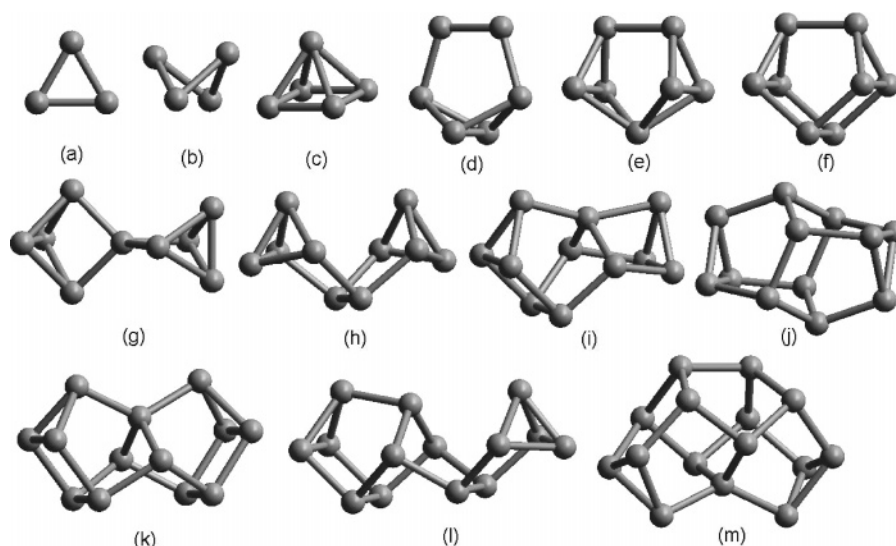


Figure 4. Ground-state geometries of cationic phosphorus clusters P_n^+ ($n = 3-15$).

$P_{13}-P_{15}$, P_4^+ , P_6^+ , P_8^+ , $P_{13}^+-P_{15}^+$, P_4^- , P_8^- , and $P_{11}^- - P_{15}^-$ as determined by Guo et al. show higher total energies and are in configurations different from those of our optimized isomers (models 3a, 3d, 3h, and 3k-3m; 4b, 4d, 4f, and 4k-4m; and 5b, 5f, and 5i-5m as depicted in Figures 3-5, respectively). In other words, the ground-state structures obtained by Guo et al. are not global minima, and the discussions conducted by them are doubtful.

At the beginning of a study, nothing was known other than the phosphorus cluster formula. The "guessing" of a reasonable geometric structure was the initial step of the optimization process. Unfortunately, there is no experimental technique that can provide direct information on cluster geometry. The only method that enables the determination of cluster geometries at present is based on comparison of the total energies after theoretical calculations. To locate the global minimum on an energy surface, it is necessary to investigate a large number of models; otherwise, the structure with the lowest energy might be missed. To date, there have been no detailed and convincing investigations of the ground states of P_n ($n = 13-15$), P_n^+ ($n = 6, 8, 10, 12-15$), and P_n^- ($n = 8, 10, 12-15$) clusters. To reduce the chance of having the ground-state structures be wrongly determined, we designed numerous models of the above

charged phosphorus clusters, including some that had never been calculated before. After geometry optimization, the total energies were compared for the determination of ground-state isomers.

For isomers that are close in energy, a difference in calculation method or basis set might result in a difference in energy order. To test the authenticity of the geometries obtained, we recalculated the ground-state isomers of previous publications at the B3LYP/6-311+G**/B3LYP/6-311G* level. Listed in Table 1 are the symmetries, electronic states, and total energies of the P_n , P_n^+ , and P_n^- ($n = 3-15$) structures with real vibrational frequencies (as displayed in Figures 3-5). In the cases of doublet-state P_n , P_n^+ , and P_n^- ($n = 3-15$) isomers, the spin contamination $\langle S^2 \rangle$ values (before annihilation of the contaminants) are between 0.753 and 0.778; such a small deviation should not have a significant effect on our results.

As displayed in Figure 3, the ground-state isomer of P_3 is triangular with C_{2v} symmetry (model 3a).^{11,28} The tetrahedral P_4 structure (model 3b) with T_d symmetry is useful for the construction of large phosphorus clusters.^{11,28} The P_5 (model 3c) of C_{2v} symmetry has a configuration derived from tetrahedral P_4 via the breaking of a bond and the addition of a two-coordinate atom.^{11,28,34} Model 3d of ground-state P_6 with C_{2v} symmetry is derived from model 3c by replacing the single atom

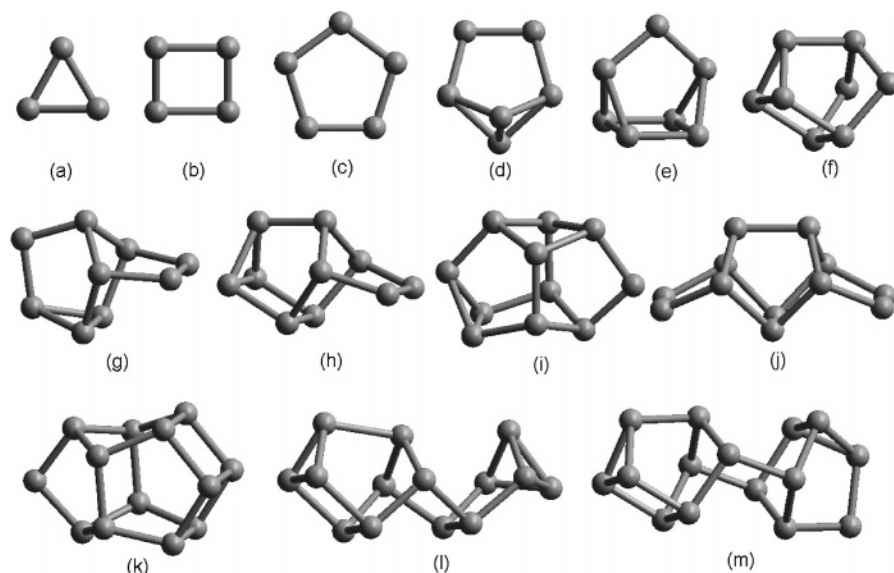


Figure 5. Ground-state geometries of anionic phosphorus clusters P_n^- ($n = 3-15$).

TABLE 1: Symmetries, Electronic States, Total Energies at the B3LYP/6-311G* and B3LYP/6-311+G* Levels, Zero-Point Energies (ZPE), and Total Energies at the B3LYP/6-311+G* with the ZPE Level of Ground-State P_n , P_n^+ , and P_n^- ($n = 3-15$) Clusters^a

model	cluster	symmetry	state	total energy (6-311G*)	total energy (6-311+G*)	ZPE	total energy (6-311+G* with ZPE)
3a	P_3	C_{2v}	2A_2	-1024.090 81	-1024.096 48	0.002 77	-1024.093 71
3b	P_4	T_d	1A_1	-1365.528 26	-1365.535 49	0.006 12	-1365.529 37
3c	P_5	C_{2v}	2B_1	-1706.863 07	-1706.872 05	0.007 48	-1706.864 57
3d	P_6	C_{2v}	1A_1	-2048.267 53	-2048.278 23	0.009 56	-2048.268 67
3e	P_7	C_{2v}	2B_1	-2389.645 04	-2389.658 14	0.011 19	-2389.646 95
3f	P_8	C_{2v}	1A_1	-2731.041 92	-2731.057 59	0.013 64	-2731.043 94
3g	P_9	C_s	$^2A''$	-3072.414 65	-3072.436 17	0.015 03	-3072.421 14
3h	P_{10}	C_{2v}	1A_1	-3413.826 61	-3413.848 08	0.017 51	-3413.830 58
3i	P_{11}	C_s	$^2A'$	-3755.198 23	-3755.225 36	0.019 28	-3755.206 08
3j	P_{12}	D_{3d}	$^1A_{1g}$	-4096.601 23	-4096.633 51	0.021 53	-4096.611 98
3k	P_{13}	C_s	$^2A'$	-4437.954 64	-4437.988 52	0.022 76	-4437.965 76
3l	P_{14}	C_s	$^1A'$	-4779.384 30	-4779.418 84	0.025 52	-4779.393 32
3m	P_{15}	C_s	$^2A''$	-5120.746 36	-5120.784 67	0.027 02	-5120.757 65
4a	P_3^+	D_{3h}	$^1A'$	-1023.809 04	-1023.814 68	0.003 66	-1023.811 02
4b	P_4^+	C_{2v}	2A_1	-1365.193 27	-1365.201 15	0.005 51	-1365.195 64
4c	P_5^+	C_{4v}	1A_1	-1706.597 40	-1706.606 42	0.007 75	-1706.598 67
4d	P_6^+	C_{2v}	2B_1	-2047.959 05	-2047.971 94	0.008 96	-2047.962 99
4e	P_7^+	C_{2v}	1A_1	-2389.372 10	-2389.386 72	0.011 26	-2389.375 46
4f	P_8^+	C_{2v}	2A_2	-2730.745 36	-2730.762 85	0.012 83	-2730.750 02
4g	P_9^+	D_{2d}	1A_1	-3072.165 19	-3072.182 38	0.016 05	-3072.166 33
4h	P_{10}^+	C_s	$^2A'$	-3413.523 82	-3413.548 13	0.016 67	-3413.531 46
4i	P_{11}^+	C_s	$^1A'$	-3754.922 81	-3754.950 09	0.019 74	-3754.930 35
4j	P_{12}^+	C_i	2A_g	-4096.300 02	-4096.338 41	0.020 13	-4096.318 29
4k	P_{13}^+	C_{2v}	1A_1	-4437.720 08	-4437.752 54	0.024 06	-4437.728 48
4l	P_{14}^+	C_s	2A	-4779.081 26	-4779.120 55	0.023 86	-4779.096 69
4m	P_{15}^+	C_{2v}	1A_1	-5120.477 59	-5120.521 01	0.027 45	-5120.493 56
5a	P_3^-	D_{3h}	$^3A'$	-1024.156 82	-1024.162 23	0.003 10	-1024.159 13
5b	P_4^-	D_{2h}	$^2B_{1g}$	-1365.548 26	-1365.554 16	0.004 90	-1365.549 26
5c	P_5^-	D_{5h}	$^1A_1'$	-1707.006 94	-1707.012 86	0.007 67	-1707.005 19
5d	P_6^-	C_{2v}	2A_2	-2048.351 50	-2048.359 52	0.009 12	-2048.350 41
5e	P_7^-	C_{2v}	1A_1	-2389.758 57	-2389.768 01	0.011 40	-2389.756 61
5f	P_8^-	C_s	2A	-2731.134 63	-2731.147 31	0.012 85	-2731.134 46
5g	P_9^-	C_s	$^1A'$	-3072.541 81	-3072.558 59	0.015 20	-3072.543 40
5h	P_{10}^-	C_s	$^2A''$	-3413.919 15	-3413.939 01	0.017 04	-3413.921 97
5i	P_{11}^-	C_s	$^1A'$	-3755.316 94	-3755.339 80	0.019 13	-3755.320 67
5j	P_{12}^-	C_{2v}	2B_2	-4096.691 77	-4096.717 67	0.020 60	-4096.697 07
5k	P_{13}^-	C_{2v}	1A_1	-4438.079 68	-4438.109 13	0.022 75	-4438.086 38
5l	P_{14}^-	C_s	$^2A'$	-4779.459 79	-4779.488 97	0.023 85	-4779.465 12
5m	P_{15}^-	C_s	$^1A'$	-5120.876 43	-5120.909 56	0.027 08	-5120.882 48

^a All energies are in a.u.

at the top with a diatomic unit.^{10,11,28,29} Model 3e with C_{2v} symmetry is the P_7 isomer derived from a boat-shaped P_6 structure by adding a two-coordinate atom at the top.³⁴ Model

3f (P_8) with C_{2v} symmetry is the well-known cuneane structure that is a common subunit of large phosphorus clusters.^{10,11,19,30,36} The ground-state isomer of P_9 (model 3g) with C_s symmetry is

derived from model 3e by breaking one bond and then adding two two-coordinate atoms.^{12,34} The structure of P₁₀ (model 3h) with C_{2v} symmetry is derived from two tetrahedral P₄ units by connecting a P₂ unit to them.^{10,13,16,31} The ground-state P₁₁ structure (model 3i) with C_s symmetry is derived from a cuneane P₈ and a triangular P₃ linked together by two single bonds.³⁵ Model 3j (P₁₂) with D_{3d} symmetry is the result of merging two cuneane P₈ units via the sharing of four atoms.^{10,16,32} Model 3k with C_s symmetry is the structure of ground-state P₁₃ derived from model 3i by breaking one bond and adding two two-coordinate atoms at the left side.³³ The structure of P₁₄ (model 3l) with C_s symmetry is derived from a cuneane P₈ unit and a tetrahedral P₄ unit by connecting them with a P₂ unit via four single bonds. Model 3m of P₁₅ with C_s symmetry is derived from models 3e and 3f by connecting them together via breaking and re-forming two bonds.

Shown in Figure 4 are the ground-state isomers of P_n⁺ (*n* = 3–15). Model 4a is triangular P₃⁺ structure with D_{3h} symmetry. Model 4b is a “butterfly”-shaped P₄⁺ unit with C_{2v} symmetry. The P₅⁺ structure (model 4c) with C_{4v} symmetry exhibits a square-pyramidal configuration.^{4,12,34} Model 4d (P₆⁺) with C_{2v} symmetry has a configuration similar to that of neutral P₆ (model 3d). Model 4e (P₇⁺) with C_{2v} symmetry is derived from a square-face-capped triangular prism by the breaking of two bonds.^{4,12,34} The isomer of P₈⁺ (model 4f) with C_{2v} symmetry has a configuration similar to that of neutral cuneane P₈ (model 3f). Ground-state P₉⁺ (model 4g) is a D_{2d} structure with a four-coordinate atom shared between two tetrahedral P₄ unit.³⁴ Model 4h of P₁₀⁺ with C_s symmetry has a configuration similar to that of ground-state neutral P₁₀ (model 3h). Model 4i of P₁₁⁺ is a C_s structure derived from neutral P₁₁ (model 3i) by bonding the two-coordinate atom to the atom on the upper right, making the latter a four-coordinate atom.^{12,35} The configuration of P₁₂⁺ (model 4j) with C_i symmetry is similar to that of neutral P₁₂ (model 3j). Model 4k (P₁₃⁺) with C_{2v} symmetry is derived from two cuneane P₈ units by sharing three side atoms. Model 4l (P₁₄⁺) with C_s symmetry has a configuration similar to that of neutral P₁₄ (model 3l). Model 4m of P₁₅⁺ with C_{2v} symmetry is a cage structure containing a four-coordinate atom at the bottom.

Shown in Figure 5 are the ground-state isomers of P_n[−] (*n* = 3–15). Model 5a is triangular P₃[−] with D_{3h} symmetry.²⁸ Model 5b of P₄[−] is a planar rectangular structure with D_{2h} symmetry.^{14,28} The isomer of P₅[−] (model 5c) is a planar pentagonal structure with D_{5h} symmetry.^{14,28,34} The P₆[−] structure with C_{2v} symmetry (model 5d) shows a configuration similar to those of neutral P₆ and cationic P₆⁺ (models 3d and 4d).^{14,28} Model 5e (P₇[−]) with C_{2v} symmetry displays a configuration similar to that of neutral P₇ (model 3e).^{14,34} The structure of P₈[−] with C_{2v} symmetry (model 5f) is derived from a neutral cuneane P₈ unit by the breaking of one bond.¹⁴ The isomer of P₉[−] (model 5g) shows a configuration similar to that of neutral P₉ (model 3g).^{14,34} The P₁₀[−] structure (model 5h) with C_s symmetry is derived from a cuneane P₈ unit by opening the P–P bond at the right and adding a P₂ unit. The structure of P₁₁[−] (model 5i) with C_s symmetry appears to be a cage structure with one two-coordinate atom.³⁵ The P₁₂[−] structure (model 5j) with C_{2v} symmetry is derived from model 5h (P₁₀[−]) by adding a P₂ unit at the left. Model 5k (P₁₃[−]) with C_s symmetry is derived from a pentagonal prism via the breaking of two bonds and the adding of three atoms. Model 5l (P₁₄[−]) with C_s symmetry has a configuration similar to those of neutral P₁₄ (model 3l) and cationic P₁₄⁺ (model 4l). Model 5m (P₁₅[−]) with C_s symmetry has a configuration similar to that of P₁₅ (model 3m).

TABLE 2: Energy Differences (ΔE_n^+), Ionization Potentials (IP), Atomization Energies (ΔE_a^+), and Incremental Binding Energies (ΔE^{I+}) of Ground-State P_n⁺ (*n* = 3–15) Clusters^a

cluster	ΔE_n^+	IP	ΔE_a^+	ΔE^{I+}
P ₃ ⁺		0.282 69	−0.034 17	
P ₄ ⁺	−341.384 62	0.333 73	0.068 72	0.102 89
P ₅ ⁺	−341.403 02	0.265 90	0.190 02	0.121 30
P ₆ ⁺	−341.364 32	0.305 69	0.272 61	0.082 59
P ₇ ⁺	−341.412 48	0.271 49	0.403 35	0.130 74
P ₈ ⁺	−341.374 55	0.293 93	0.496 18	0.092 83
P ₉ ⁺	−341.416 31	0.254 80	0.630 76	0.134 58
P ₁₀ ⁺	−341.365 12	0.299 12	0.714 16	0.083 40
P ₁₁ ⁺	−341.398 90	0.275 73	0.831 32	0.117 16
P ₁₂ ⁺	−341.387 93	0.293 69	0.937 53	0.106 21
P ₁₃ ⁺	−341.410 19	0.237 28	1.065 98	0.128 45
P ₁₄ ⁺	−341.368 21	0.296 63	1.152 46	0.086 48
P ₁₅ ⁺	−341.396 87	0.264 09	1.267 60	0.115 14

^a All energies are in a.u.

According to Figures 1–3, a number of neutral, cationic, and anionic P_n clusters are similar in configuration while differing in geometric parameters (bond length, bond angle, and torsion angle). For example, the ground-state P_n and P_n[−] (*n* = 3, 6, 7, 8, 9, 14, and 15) clusters show similar configurations. For P_n and P_n⁺ clusters, the even-*n* (*n* = 6, 8, 10, 12, and 14) isomers exhibit similar configurations. It is apparent that when there is a change in charge, a phosphorus cluster of odd *n* stands a higher chance of undergoing obvious change in structural configuration. There exists an interesting trend that cationic P_n⁺ (*n* = 5, 7, 9, 11, 13) clusters prefer to adopt a structure with an atom in four-fold coordination. In those cases, all orbitals are fully involved in bonding.⁴

Phosphorus has a chemistry that transcends the traditional boundaries of inorganic chemistry. In the ground state, phosphorus exhibits an electronic configuration of [Ne]3s²3p_x¹3p_y¹3p_z¹ with three unpaired electrons, and with low-lying vacant 3d orbitals available, the various forms of elemental phosphorus can interconvert under suitable heat and pressure treatments.² The P_n, P_n⁺, and P_n[−] (*n* = 3–15) structures exhibit a variety of configurations, including planar, tetrahedral, cuneane, and cage, many of which are polymeric forms of the tetrahedral P₄ and/or cuneane P₈ subunits. Models 3c, 3d, 3h, 3i, 4d, 4e, 4g, 4h, 4l, 5d, and 5l contain tetrahedral P₄ as subunits. Models 3g, 3i–3m, 4i–4l, 5g–5j, 5l and 5m are all derived from the cuneane P₈ configuration. It is obvious that both tetrahedral P₄ and cuneane P₈ units are favorable components for the construction of large clusters.

3.2 Energy Differences. To evaluate the relative stabilities of the clusters of various sizes, the energy difference, defined as the difference between the total energies of the adjacent clusters, was calculated. For cationic and anionic clusters the energy difference were determined as:

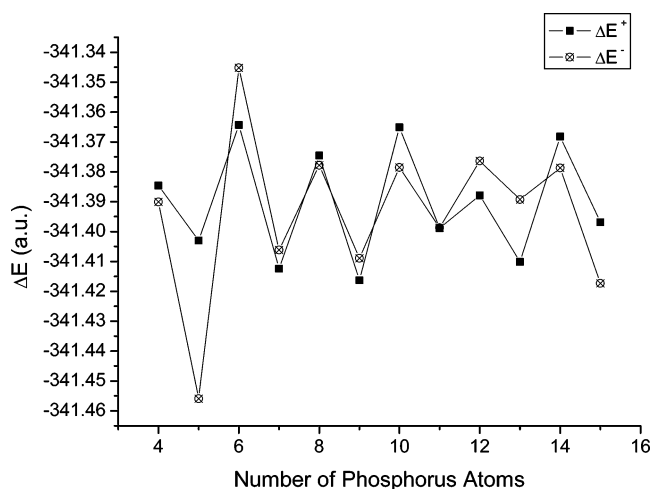
$$\Delta E_n^+ = E(\text{P}_n^+) - E(\text{P}_{n-1}^+) \quad \text{for cationic clusters}$$

$$\Delta E_n^- = E(\text{P}_n^-) - E(\text{P}_{n-1}^-) \quad \text{for anionic clusters}$$

Listed in Table 2 are the energy differences (ΔE_n^+), ionization potentials (IP), atomization energies (ΔE_a^+), and incremental binding energies (ΔE^{I+}) with zero-point energy corrections of the ground-state cationic P_n⁺ (*n* = 3–15) clusters. Listed in Table 3 are the energy differences (ΔE_n^-), electron affinities (EA), atomization energies (ΔE_a^-), and incremental binding energies (ΔE^{I-}) with zero-point energy corrections of the ground-state P_n[−] (*n* = 3–15) clusters. Displayed in Figure 6 are the variations in the energy differences (ΔE_n^+ and ΔE_n^-)

TABLE 3: Energy Differences (ΔE_n^-), Electron Affinities (EA), Atomization Energies (ΔE_a^-), and Incremental Binding Energies ($\Delta E^{I\pm}$) of Ground-State Anionic P_n^- ($n = 3-15$) Clusters^a

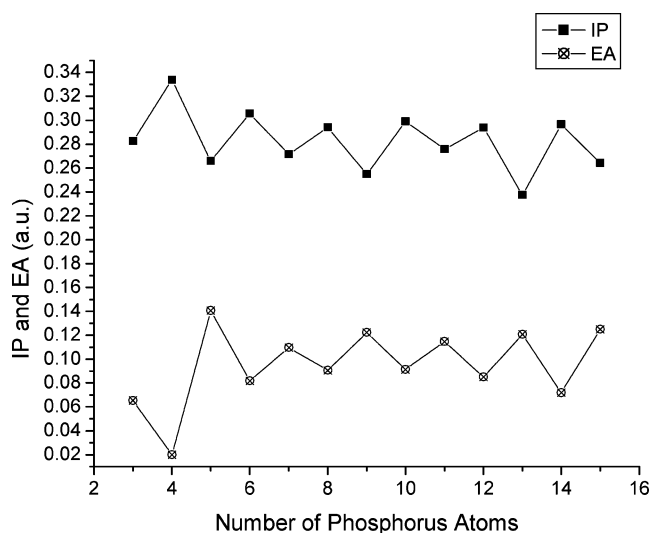
cluster	ΔE_n^-	EA	ΔE_a^-	ΔE^{I-}
P_3^-		0.065 42	0.313 94	
P_4^-	-341.390 13	0.019 89	0.422 34	0.108 40
P_5^-	-341.455 94	0.140 62	0.596 54	0.174 20
P_6^-	-341.345 21	0.081 73	0.660 03	0.063 49
P_7^-	-341.406 20	0.109 65	0.784 50	0.124 47
P_8^-	-341.377 86	0.090 52	0.880 62	0.096 12
P_9^-	-341.408 94	0.122 26	1.007 83	0.127 21
P_{10}^-	-341.378 57	0.091 39	1.104 67	0.096 84
P_{11}^-	-341.398 70	0.114 58	1.221 64	0.116 97
P_{12}^-	-341.376 40	0.085 09	1.316 31	0.094 67
P_{13}^-	-341.389 32	0.120 63	1.423 89	0.107 58
P_{14}^-	-341.378 74	0.071 80	1.520 89	0.097 01
P_{15}^-	-341.417 36	0.124 83	1.656 52	0.135 63

^a All energies are in a.u.**Figure 6.** Variations in energy differences of ground-state P_n^+ and P_n^- ($n = 3-15$) clusters versus the number of phosphorus atoms n .

of ground-state P_n^+ and P_n^- ($n = 3-15$) clusters versus the number of phosphorus atoms. According to the characteristic odd/even alternation, the clusters with odd n have lower ΔE_n^+ and ΔE_n^- values than the adjacent clusters with even n , showing that the clusters with odd n are more stable than those with even n .

3.3 Ionization Potentials and Electron Affinity. Ionization potential (IP, adiabatic), defined as the amount of energy required to remove an electron from a molecule, is calculated as the energy difference between the optimized cation and neutral molecule (i.e., $E_{\text{optimized cation}} - E_{\text{optimized neutral}}$). A lower ionization potential means that less energy is needed to remove an electron from the neutral molecule and the generation of the corresponding cationic isomer is more feasible. A cationic cluster with a smaller ionization potential is generally more stable. Thus, ionization potential can be used as a criterion to evaluate the relative stabilities of cationic clusters of different sizes.

Electron affinity (EA, adiabatic), defined as the energy released when an electron is added to a neutral molecule, is calculated as the energy difference between the optimized neutral and anionic molecules (i.e., $E_{\text{optimized neutral}} - E_{\text{optimized anion}}$). A higher electron affinity means that more energy is released when an electron is added to the neutral molecule and the generation of the corresponding anion is more readily achieved. An anionic cluster with a higher electron affinity is generally more stable. Therefore, electron affinity can be used

**Figure 7.** Ionization potentials (IP, au) and electron affinity (EA, au) of ground-state P_n^+ and P_n^- ($n = 3-15$) clusters versus the number (n) of phosphorus atoms.

as a criterion to evaluate the relative stabilities of anionic clusters of different sizes.

Figure 7 depicts the variations of the ionization potentials (IP) and electron affinities (EA) of the ground-state P_n^+ and P_n^- ($n = 3-15$) clusters versus the number of phosphorus atoms n . One can see that the IP values of P_n^+ with odd n are lower than those with even n , reflecting an alternating pattern of high and low. This implies that, compared to clusters of even n , it is easier to lose an electron from P_n when n is odd. There is a parity effect on the EA curve of P_n^- : EA values of odd- n clusters are higher than those of adjacent even- n clusters. This behavior reflects the higher stability of the odd- n P_n^- ($n = 3-15$) clusters.

3.4 Incremental Binding Energy. The incremental binding energy (ΔE^{I+} and ΔE^{I-}), which is the difference in atomization energy (ΔE_a^+ and ΔE_a^-) of adjacent clusters, can also reflect the relative stabilities of cationic and anionic clusters.⁴⁴ It is expressed as

$$\Delta E^{I+} = \Delta E_a^+(P_n^+) - \Delta E_a^+(P_{n-1}^+) \quad \text{for cationic clusters}$$

$$\Delta E^{I-} = \Delta E_a^-(P_n^-) - \Delta E_a^-(P_{n-1}^-) \quad \text{for anionic clusters}$$

where ΔE_a is defined as the energy difference between a molecule and its component atoms

$$\Delta E_a^+ = nE(P) - E(P_n^+) \quad \text{for cationic clusters}$$

$$\Delta E_a^- = nE(P) - E(P_n^-) \quad \text{for anionic clusters}$$

Figure 8 displays the incremental binding energies (ΔE^{I+} and ΔE^{I-}) of the ground-state P_n^+ and P_n^- ($n = 3-15$) clusters versus the number of phosphorus atoms n . One can see that the values of ΔE^{I+} vary according to a pattern of odd/even alternation: When n is odd, the ΔE_n^{I+} value is large; when n is even, the ΔE_n^{I+} value is small. Because a larger ΔE^{I+} value implies a more stable P_n^+ structure, one can deduce that a P_n^+ cluster with odd n is more stable than one with even n . There is also a parity effect on the ΔE^{I-} curve of P_n^- : ΔE^{I-} values of odd- n clusters are higher than those of adjacent even- n anions. This behavior again reflects the higher stability of the odd- n P_n^- ($n = 3-15$) clusters.

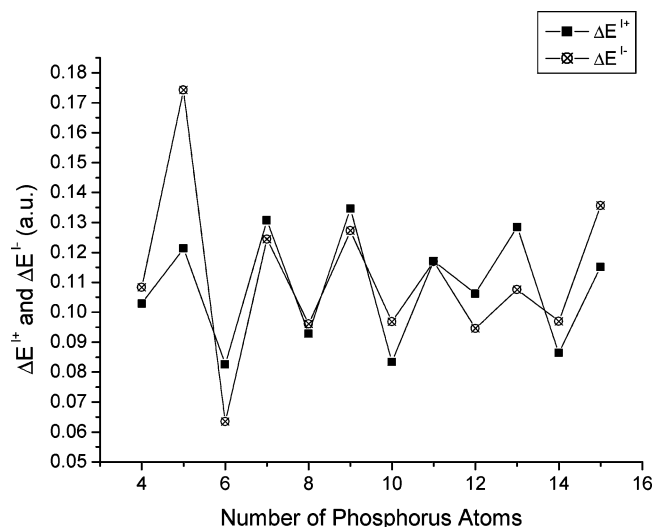


Figure 8. Incremental binding energies (ΔE^{+} and ΔE^{-} , au) of ground-state P_n^{+} and P_n^{-} ($n = 3-15$) clusters versus the number (n) of phosphorus atoms.

The odd/even alternation of TOF mass signal intensities reflects the mass distribution of positive and negative phosphorus clusters. The alternation effect is a result of the structure of the ions. Such an alternating odd/even pattern of energy differences, ionization potentials, electron affinities, and incremental binding energies is consistent with the experimental results depicted in Figures 1 and 2.⁵

4. Conclusions

We have conducted a comprehensive B3LYP study on neutral, cationic, and anionic phosphorus clusters with sizes $n = 3-15$. The stabilities of the clusters exhibit obvious even/odd alternations. The cationic and anionic clusters with odd n are more stable than those with even n . The trend of odd/even alternation can be rationalized on the basis of the variations in energy difference, ionization potential, electron affinity, and incremental binding energy. The results of the calculations are in good agreement with the relative intensities observed in the time-of-flight mass spectra of cationic and anionic phosphorus clusters.

Acknowledgment. This work was supported by the National Science Foundation of China (Grant 20473061 and 20533020).

References and Notes

- Weltner, W.; Van Zee, R. J., Jr. *Chem. Rev.* **1989**, *89*, 1713.
- Greenwood, N. N.; Earnshaw, A. *Chemistry of the Elements*; Pergamon Press: Oxford, U.K., 1985.
- Martin, T. P. *Z. Phys. D* **1986**, *3*, 211.
- Huang, R. B.; Li, H. D.; Lin, Z. Y.; Yang, S. H. *J. Phys. Chem.* **1995**, *99*, 1418.
- Liu, Z. Y.; Huang, R. B.; Zheng, L. S. *Z. Phys. D* **1996**, *38*, 171.
- Bulgakov, A. V.; Bobrenok, O. F.; Kosyakov, V. I. *Chem. Phys. Lett.* **2000**, *320*, 19.
- Bulgakov, A. V.; Bobrenok, O. F.; Kosyakov, V. I.; Ozerov, I.; Marine, W.; Heden, M.; Rohmund, F.; Campbell, E. E. B. *Phys. Solid State* **2002**, *44* (4), 617.
- Bulgakov, A. V.; Bobrenok, O. F.; Ozerov, I.; Marine, W.; Giorgio, S.; Lassesson, A.; Campbell, E. E. B. *Appl. Phys. A* **2004**, *79* (4-6), 1369.
- Šedo, O.; Voráč, Z.; Alberti, M.; Havel, J. *Polyhedron* **2004**, *23*, 1199.
- Ahlich, R.; Brode, S.; Ehrhardt, C. *J. Am. Chem. Soc.* **1985**, *107*, 7260.
- Jones, R. O.; Hohl, D. *J. Chem. Phys.* **1990**, *92*, 6710.
- Jones, R. O.; Seifert, G. *J. Chem. Phys.* **1992**, *96*, 7564.
- Ballone, P.; Jones, R. O. *J. Chem. Phys.* **1994**, *100*, 4941.
- Jones, R. O.; Ganteför, G.; Hunsicker, S.; Pieperhoff, P. *J. Chem. Phys.* **1995**, *103*, 9549.
- Häser, M.; Schneide, U.; Ahlich, R. *J. Am. Chem. Soc.* **1992**, *114*, 9551.
- Häser, M.; Treutler, O. *J. Chem. Phys.* **1995**, *102*, 3703.
- Häser, M. *J. Am. Chem. Soc.* **1994**, *116*, 6925.
- Warren, D. S.; Gimarc, B. M. *J. Am. Chem. Soc.* **1992**, *114*, 5378.
- Gimarc, B. M.; Warren, D. S. *Inorg. Chem.* **1993**, *32*, 1850.
- Feng, J. N.; Cui, M.; Huang, X. R.; Otto, P.; Gu, F. L. *J. Mol. Struct. (THEOCHEM)* **1998**, *425*, 201.
- Feng, J. N.; Huang, X. R.; Li, Z. S.; Sun, C. C.; Zhang, G. *Chem. J. Chin. Univ.* **1996**, *17*, 1112.
- Huang, X. R.; Feng, J. N.; Li, Z. S.; Sun, C. C.; Zhang, G. *Chem. J. Chin. Univ.* **1996**, *17*, 1116.
- Huang, X. R.; Feng, J. N.; Li, Z. S.; Sun, C. C.; Zhang, G. *Chem. J. Chin. Univ.* **1996**, *17*, 930.
- Feng, J. N.; Huang, X. R.; Li, Z. S.; Sun, C. C.; Zhang, G. *Chem. J. Chin. Univ.* **1996**, *17*, 1273.
- Feng, J. N.; Huang, X. R.; Sun, C. C. *Chem. J. Chin. Univ.* **1997**, *18*, 1112.
- Guo, L.; Wu, H. S.; Jin, Z. H. *J. Mol. Struct. (THEOCHEM)* **2004**, *677*, 59.
- Han, J. G.; Morales, J. A. *Chem. Phys. Lett.* **2004**, *396* (1-3), 27.
- Wang, D.; Xiao, C. L.; Xu, W. G. *J. Mol. Struct. (THEOCHEM)* **2004**, *759*, 225.
- Chen, M. D.; Luo, H. B.; Qiu, Z. J.; Huang, R. B.; Zheng, L. S.; Au, C. T. *Chin. J. Struct. Chem.* **2000**, *19* (4), 311.
- Chen, M. D.; Huang, R. B.; Zheng, L. S.; Au, C. T. *J. Mol. Struct. (THEOCHEM)* **2000**, *499*, 195.
- Chen, M. D.; Luo, H. B.; Li, J. T.; Qiu, Z. J.; Huang, R. B.; Zheng, L. S.; Au, C. T. *Chin. J. Chem. Phys.* **2000**, *13* (3), 281.
- Chen, M. D.; Luo, H. B.; Qiu, Z. J.; Zhang, Q. E.; Au, C. T. *Main Group Metal Chem.* **2000**, *23* (5), 291.
- Liu, M. H.; Jiao, Y. C.; Liu, J. W.; Chen, M. D.; Zhang, Q. E. *J. Xiamen Univ.* **2003**, *42* (3), 331.
- Chen, M. D.; Huang, R. B.; Zheng, L. S.; Zhang, Q. E.; Au, C. T. *Chem. Phys. Lett.* **2000**, *325*, 22.
- Chen, M. D.; Luo, H. B.; Liu, M. H.; Zhang, Q. E.; Au, C. T. *Main Group Metal Chem.* **2000**, *23* (8), 361.
- Chen, M. D.; Li, J. T.; Huang, R. B.; Zheng, L. S.; Au, C. T. *Chem. Phys. Lett.* **1999**, *305*, 439.
- HyperChem Reference Manual*; Hypercube Inc.: Waterloo, Ontario, Canada, 1996.
- James, M.; Crabbe, C.; Appleyard, J. R.; Lay, J. R. *Desktop Molecular Modeller*; Oxford University Press: Oxford, U.K., 1994.
- Frisch, M. J.; Trucks, G. W.; Schlegel, H. B.; Scuseria, G. E.; Robb, M. A.; Cheeseman, J. R.; Zakrzewski, V. G.; Montgomery, J. A., Jr.; Stratmann, R. E.; Burant, J. C.; Dapprich, S.; Millam, J. M.; Daniels, A. D.; Kudin, K. N.; Strain, M. C.; Farkas, O.; Tomasi, J.; Barone, V.; Cossi, M.; Cammi, R.; Mennucci, B.; Pomelli, C.; Adamo, C.; Clifford, S.; Ochterski, J.; Petersson, G. A.; Ayala, P. Y.; Cui, Q.; Morokuma, K.; Salvador, P.; Dannenberg, J. J.; Malick, D. K.; Rabuck, A. D.; Raghavachari, K.; Foresman, J. B.; Cioslowski, J.; Ortiz, J. V.; Baboul, A. G.; Stefanov, B. B.; Liu, G.; Liashenko, A.; Piskorz, P.; Komaromi, I.; Gomperts, R.; Martin, R. L.; Fox, D. J.; Keith, T.; Al-Laham, M. A.; Peng, C. Y.; Nanayakkara, A.; Challacombe, M.; Gill, P. M. W.; Johnson, B.; Chen, W.; Wong, M. W.; Andres, J. L.; Gonzalez, C.; Head-Gordon, M.; Replogle, E. S.; Pople, J. A. *Gaussian 98*, revision A.11; Gaussian, Inc.: Pittsburgh, PA, 2001.
- Becke, A. D. *J. Chem. Phys.* **1993**, *98*, 5648.
- Lee, C.; Yang, W.; Parr, R. G. *Phys. Rev. B* **1988**, *37*, 785.
- Foresman, J. B.; Frisch, M. J. *Exploring Chemistry with Electronic Structure Methods*; Gaussian Inc.: Pittsburgh, PA, 1996.
- Clack, T. *A Handbook of Computational Chemistry*; John Wiley and Sons: New York, 1985.
- Pascoli, G.; Lavendy, H. *Int. J. Mass Spectrom. Ion Processes* **1998**, *173*, 41.